INFLUENCE OF WELDING ON THE STRENGTH OF HIGH PERFORMANCE STEELS

Xing-Zhao Zhang[1], Ming-Shan Zhao[2], Sing-Ping Chiew[3], Chi-King Lee[4] and Tat-Ching Fung[5]

ABSTRACT: *In this study, experiments were carried out to investigate the influence of welding on the strength of high performance steels including the reheated, quenched and tempered (RQT) high strength steel in grade S690 and thermos-mechanically controlled processed (TMCP) normal strength steel in grade S385. Firstly, a special welding program was designed and performed on the RQT and TMCP steel plates to induce welding heat input to the materials. These welding affected plates were subsequently fabricated into smaller specimens for tensile test and metallurgical examination including microstructure observation and Vickers hardness test. Secondly, two T-stub joints made of these two material were manufactured and tested in tension. By comparing the first yield resistances of the T-stub specimens and the design plastic resistances obtained by using equations provided by EC3, the strength of the high performance steel T-stub joints are evaluated. The results showed that welding softened the heat affected zone (HAZ) of S690 high strength steel significantly but its effect on the normal strength steel S385 was insignificant.*

KEYWORDS: Influence of welding, strength, microstructure, hardness, high performance steel

[1] Xing-Zhao Zhang, School of Civil and Environmental Engineering, Nanyang Technological University, Singapore. Email: N1609476D@ntu.edu.sg
[2] Ming-Shan Zhao, School of Civil and Environmental Engineering, Nanyang Technological University, Singapore. Email: mszhao@ntu.edu.sg
[3] Sing-Ping Chiew, Professor of Civil Engineering, Singapore Institute of Technology, Singapore. Email: SingPing.Chiew@SingaporeTech.edu.sg
[4] Chi-King Lee, School of Engineering and Information Technology, University of New South Wales Canberra, Austrailia. Email: c.lee@adfa.edu.au
[5] Tat-Ching Fung, School of Civil and Environmental Engineering, Nanyang Technological University, Singapore. Email: ctcfung@ntu.edu.sg

1 INTRODUCTION

Primary characteristics of structural steels include mechanical and chemical properties, metallurgical structures and weldability [1]. In many applications, the main focus has tended to be only on the tensile properties (yield stress and ultimate tensile stress), with some attention paid to the deformability (elongation at fracture). Recently, after many disasters involving fatigue failure, earthquake, serious fire and terrorism attack, these commonly acceptable criteria became more frequently questioned and other performance-improving properties received more and more attentions. Modern high performance structural steels are usually the product of advanced heat treatment and characterized by increased strength and toughness together with low carbon equivalents [2]. Different from high alloy steels, the weldability of heat treated steels is improved significantly in the sense of reduced pre-heating requirements and reduced susceptibility to cold cracking [3]. As a result, higher design flexibility and construction productivity can be achieved.

For conventional steels, it is suggested that if the width of the soft zone does not exceed 25% of the plate thickness, the local softening would not necessarily impair the global strength due to the constraints of the stronger weld metal and unaffected base metal [4, 5]. However, this criterion may not apply on high performance steels, because their main constitutes in the microstructures, such as martensite and bainite, are not stable at high temperatures [6]. There is a possibility that the enhanced mechanical properties acquired by means of hardening may deteriorate significantly after exposure to heat, due to microstructural changes at certain critical temperatures [7, 8]. This undesirable property was first confirmed for work hardened cold-formed hollow sections [9], and then later for high strength steel S460 and S690 [10] and cold rolled steel Bisplate 500 [11]. Accordingly, it is not surprising that concerns are raised about the performance of welded high performance steel connections, especially when large energy input welding is applied [12].

The main objective of this paper is to experimentally investigate the influence of welding on the strength of two relatively new high performance structural steels, namely the reheated, quenched and tempered (RQT) high strength steel in grade S690 and the thermo-mechanically controlled processed (TMCP) normal strength steel in grade S385. In the first phase of this study, a special welding program was designed and performed on the RQT and TMCP steel plates to induce welding heat input to the materials. These welding affected plates were subsequently fabricated into smaller specimens for tensile test and metallurgical examination including microstructure observation and micro-hardness test. The second phase of this study investigated the tensile performance of welded T-stub joints that made of those two materials. Both the load-displacement curves and failure modes of the tested specimens are presented. In particular, the elastic stage stiffness, plastic resistance and plastic stage behaviour are analysed. By comparing the first yield resistances from the test results and the design plastic resistances obtained by using prediction equations provided by EC3, the strength of the high performance steel T-stub joints are evaluated.

2 MATERIAL PROPERTY STUDY

2.1 Base metal

Two grades of steels, namely the TMCP steel plates in grades S385 (thickness 16mm) and the RQT grade S690 HSS (thicknesses 16mm), are examined in this study. It should be mentioned that both the TMCP and the RQT steels are “emerging” types of materials for structural application when comparing with the commonly used NSS of gradeS355 steels or grades S235 and S275 mild steels.

TMCP is an advanced thermo-mechanical process to produce low carbon plate steels microalloyed with Ti, Nb and V. The concept of TMCP combines controlled hot rolling with accelerated cooling to form mainly bainite and ferrite in the microstructure [13]. By the merits of grain refinement, precipitation hardening and low amount of transformation hardening, TMCP enables the production of as-rolled steels with final properties that are tailored to the requirements and specifications of a particular application [14]. In addition to strength, hardness and toughness, weldability and corrosion resistance are usually made features of TMCP.

RQT is essentially a refined quenching and tempering technology. Similar to the conventional quenched and tempered steels, RQT steels also rely on the extremely fast cooling to produce martensite in the microstructure to greatly enhance the strengths [7]. However, RQT steel plates exhibit better homogeneity in through-thickness mechanical properties compared with traditional directly quenched and tempered steel plates. These RQT plates comply with the EN 10025-6 grade S690 specification [15].

The stress-strain curves and the mechanical properties of the steel plates obtained by standard coupon tensile test are shown in Fig. 1 and Table 1, respectively. From Table 1, two distinct features of RQT-S690 steel can be seen. First, this material has superior strengths compared to traditional steels. The actual yield strength of RQT-S690 is twice the

nominal yield strength of S355. Second, RQT-S690 steel is relatively brittle compared to traditional NSS and the TMCP-S385 tested in this study. For TMCP steels, it can also be seen from Table 1 that the TMCP-S385 steel literally fulfilled the mechanical property specifications of S420M/ML steel.

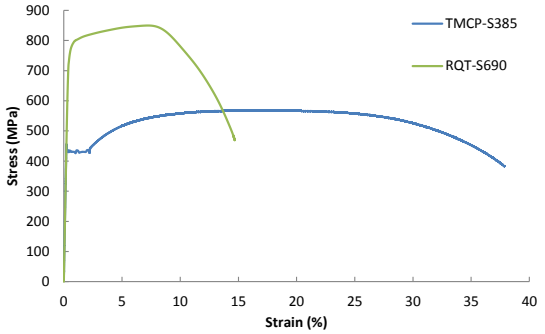

Fig. 1: *Stress-strain curves of RQT-S690 and TMCP-S385*

Table 1: *Mechanical properties of the TMCP-S385 and RQT-S690*

Strengths	f_y(MPa)	f_u(MPa)	E (GPa)	Elongation (%)
RQT-S690 (16mm)	745.2.0	837.8	208.9	14.5
EN 10025-6 S690Q/QL	690	770-940	-	14
TMCP-S385 (16mm)	443.3	568.0	208.4	37.8
EN 10025-4 S420M/ML	420	520-680	-	19

2.2 WELDING EXPERIMENTS

Theoretically, the mechanical properties of a heat affected zone (HAZ) can be assessed by direct removal of small samples from the welded joints. However, this method presents many difficulties, such as delicate positioning of the HAZ within very narrow zones with high microstructure gradients, residual stresses, etc. Instead, the properties of these zones are often assessed on the basis of experiment on test samples that undergone simulated thermal treatments representative of those encountered in the HAZ [16].

The idea of HAZ property evaluation in this study is to examine coupon specimens that have been affected by welding. In order to make the material properly affected by welding and establish well developed HAZ, a special welding process was designed: Welding was carried out on both sides of an 800mm×300mm×16 mm plate, as shown in Fig. 2. Welding was carried out in the center area of the plate along the longitudinal direction. Shielded Metal Arc Welding (SMAW) and electrode LB-70L was employed to finish the welding. The welding zone covered a full length of 100mm long. Special caution was also paid to the welding sequence to control the deformation and residual stress associated with uneven heating and cooling. Every time when two runs were finished on one side of the plate, the welding moved to the other side (Fig. 2). Fig. 3 shows the final welding affected coupon specimens.

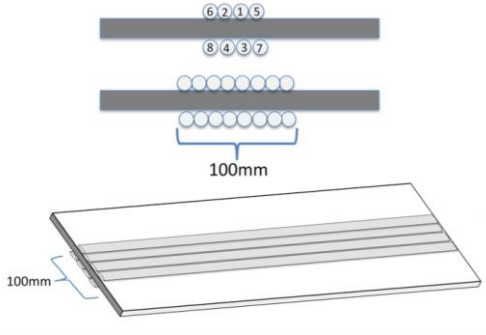

Fig. 2: *Welding program*

Fig. 3: *Coupons cut from the main plate*

2.3 MECHANICAL PROPERTY TESTS

2.3.1 Tensile test

Some welding affected coupons (Fig. 3) were further cold-grinded (Fig. 4) and fabricated into standard coupon specimens (Fig. 5). It should be noted that all the hot processes following the welding are accompanied with water cooling systems to avoid additional heat input into the specimens. For each type of steel (RQT-S690 and TMCP-S385), two specimens were tested by standard tensile test according to EN 10002-1 [17]. The loading rate was set as 1mm/min until fracture took place and data points were captured at a frequency of 1 Hz. During the tensile test, both strain gauge and extensometer were used to monitor and record the deformation.

Fig. 4: *Grinding machine with water cooling system*

Fig. 5: *Final welding affected coupon specimens*

2.3.2 Stress-strain behaviour

Figs. 6 and 7 show that tensile test results in terms of stress-strain curves of the welded affected RQT-S690 and TMCP-S385 coupons, respectively. The nominal yield strengths (the 0.2% strain offset strengths), tensile strengths, the tensile ratios as well as the strains at fracture obtained are summarized in Table 2, in which Diff1 is defined as Diff1=Welded-1 or 2/Base metal×100% (Nominal yield strength) and Diff2 is defined as Diff2=Welded-1 or 2/Base metal×100% (Tensile strength). As can be seen from Figs. 6 and 7 and Table 2, the deformation capacities of all the welded specimens in terms of elongation at fracture decreased compared with the respective base metal. The TMCP-S385 loses more deformation capacities than the RQT-S690 but gains increase in the strengths, especially yield strengths. Overall, the effect of welding on the mechanical properties of the TMCP-S385 specimens are similar to hardening effects, i.e. welding improved the strengths at the expense of ductility. It can be seen from Fig. 7 and Table 2 that the more hardening effects, the worse ductility (Specimen Welded-2). On the other hand, welding causes serious deterioration in the strengths of the RQT-S690 specimens besides the ductility. Nearly 20% of both yield and tensile strengths can be observed (Rows 3 and 4, Table 2).

2.4 METALLURGICAL EXAMINATION

In this study, both the RQT-S690 and TMCP-S385 are heat treatment hardened steels for which strength is based on non-equilibrium microstructure [18]. As a member of the QT steel family, RQT steels usually consists of meta-stable transformation microstructure of martensite or bainite, which is tempered during the production process after hardening treatment at temperatures below the transformation point A1 [7]. For TMCP, the mechanical properties are developed on the basis of fine grain microstructure which consists of mainly bainite and ferrite [5].

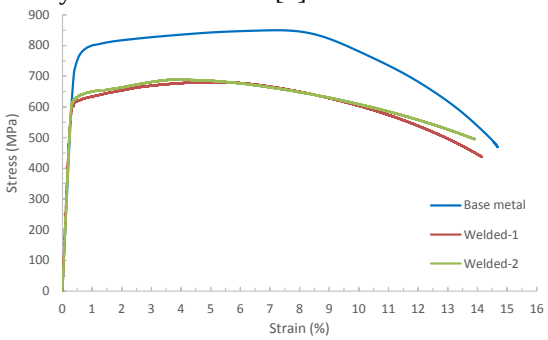

Fig. 6: *Stress-strain curves of RQT-S690*

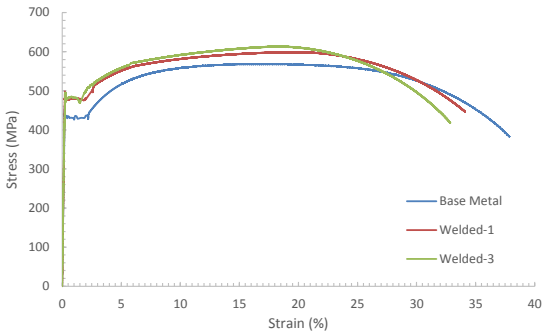

Fig. 7: *Stress-strain curves of TMCP-S385*

Theoretically, if the hardened microstructure is exposed to temperature above A_1 (727°C, for carbon steel with carbon content 0.15%) and cooled subsequently, as occurred during welding, the original hardened microstructure would transform into austenite and finally decomposes to microstructure with reduced strength, such as ferrite or upper bainite [19]. Numerous researchers have shown that thermos-mechanically treated microstructure changes irreversibly if the microstructure is exposed to temperature above A1 and transformation softening would take place [5, 19-21]. Although tempering softening is less pronounced for microalloyed TMCP steels due to a beneficial precipitation hardening effect and less transformation hardening microstructure compared

Table 2: *Mechanical Properties of RQT-S690 and TMCP-S385 after welding*

Material		Nominal yield strength (MPa)	Diff1 (%)	Tensile strength (MPa)	Diff2 (%)	Tensile ratio	*E* (GPa)	Fracture strain (%)
RQT-S690	Base metal	764.2	100	849.8	100	1.11	208.9	14.7
	Welded-1	619.5	81.1	681.2	80.1	1.10	206.9	14.1
	Welded-2	632.1	82.7	689.8	81.2	1.09	209.3	13.9
TMCP-S385	Base Metal	443.3	100	568.0	100	1.28	208.4	37.8
	Welded-1	476.6	107.5	598.4	105.4	1.31	211.0	34.1
	Welded-2	481.1	108.5	611.5	107.7	1.27	207.2	32.8

with RQT steels, the soft zone is equally inevitable for TMCP steels [5]. However, in this study, it is shown (Figs. 6 and 7 and Table 2) that only the strengths of the RQT-S690 decreased significantly after welding, while the ultimate strengths of TMCP-S385 steel was even increased. In order to further investigate the effect of welding on the RQT-S690 and TMCP-S385 steels and search the "missing" soft zone of the TMCP-S385 steel, metallurgical analysis is carried out experimentally.

2.4.1 Metallurgical examination

The metallurgical examination is conducted for the cross sections of the welding affected coupons (Fig. 3). This examination consists of two steps, i.e. (1) microstructure by light optical microscopy; and (2) Vickers hardness measurements according to ISO 6507-1 [22].

The metallurgical specimens were carefully fabricated by using the precision cutter, grinder and polisher and finally etched with nital solution. The final samples are shown in Fig. 8. As can be seen from Fig. 8, each sample contains two passes of welding and the fusion zone, HAZ and base metal zones are in strip shapes.

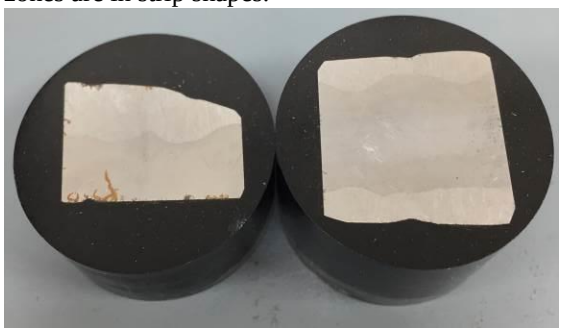

Fig. 8: *Metallurgical examination sample*

2.4.2 Microstructure and hardness

Figs. 9 and 10 show the original microstructures of the RQT-S690 and TMCP-S385, respectively. It can be seen from Figs. 9 and 10 that, in accordance with the metallurgical theory, the composition of RQT-S690 is typical lath-shaped martensite, while the TMCP-S385 consists of fine grain mixture of bainite and ferrite.

The HAZs of RQT-S690 and TMCP-S385 are shown in Figs. 11 and 12, respectively. It can be seen clearly from Figs. 11 and 12 that the grain sizes of the both HAZs are greatly increased, especially near the fusion zone. Although the grain sizes gradually decrease with the distance from the fusion zone, the sizes are still much larger than those of the base metal (Figs. 9 and 10). Depending on the microstructural changes in the HAZ, normally three sub-HAZs can be defined: (1) The coarse grained HAZ (CGHAZ), i.e. the grain enlargement zone. Temperature in this zone ranges from A3 up to the melting point (about 1500°C), (2) Fine grained HAZ (FGHAZ), i.e. the recrystallized zone and intercritical HAZ (partially transformed zone). This zone has been heated to a temperature higher than the transformation temperature A_1 but lower than A_3 (about 830°C for structural steel with carbon content 0.15%), (3) Tempering zone. The mechanical properties of this zone is not much different from the base material since no transformation phase takes place [7]. In this study, at least two of the sub-HAZs, namely the CGHAZ and FGHAZ, can be observed clearly (Figs. 11 and 12). The tempering zone is furthest from the fusion zone and is not within these two figures.

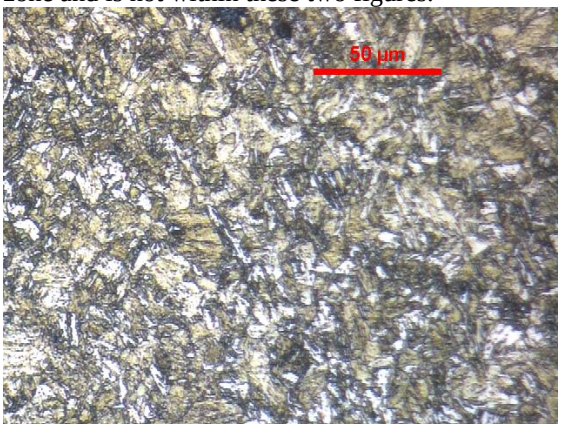

Fig. 9: *Original Microstructure of RQT-S690*

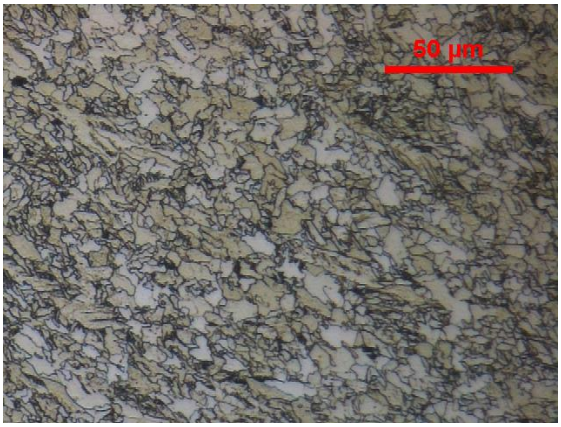

Fig. 10: *Original Microstructure of TMCP-S385*

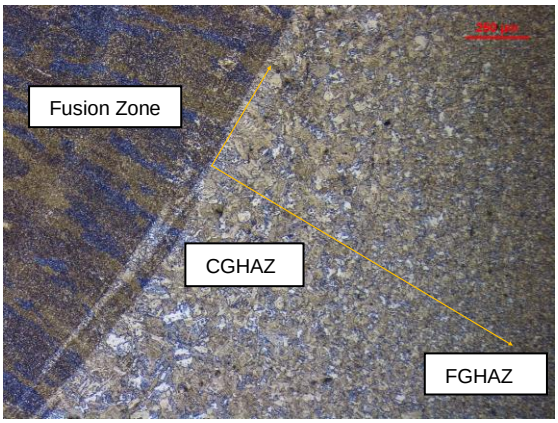

Fig. 11: *Microstructure in the HAZ of RQT-S690*

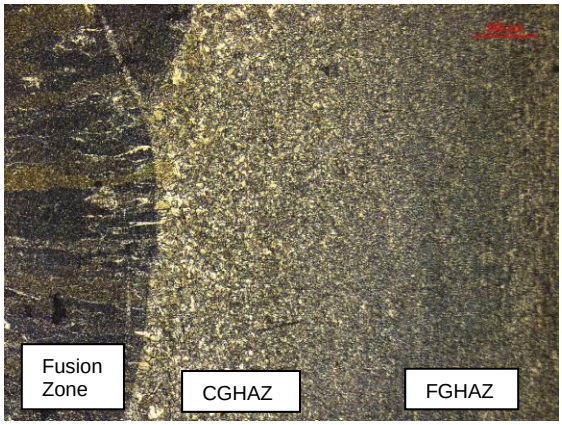

Fig. 12: *Microstructure in the HAZ of TMCP-S385*

The Vickers hardness test was carried out to measure the hardness variation from the fusion zone to the base metal. As shown in Fig. 11, the origin is set at the boundary between the fusion zone and the HAZ, since it can be clearly defined after etching. The distance between adjacent two measurement locations is 0.2mm. The measurement covered the area ranging from -2mm up to 7mm. The precision of the positioning was guaranteed by the digital x-y direction movement control stage (Fig. 13). For all the samples, 500g indentation force was adopted in the tests.

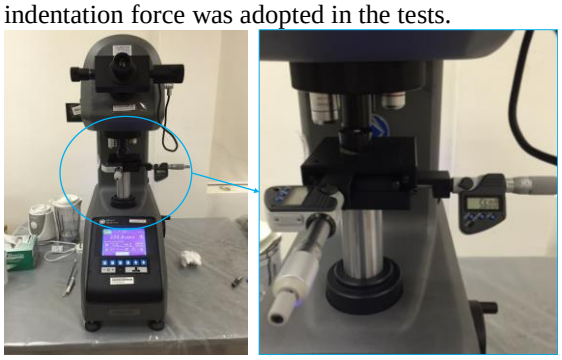

Fig. 13: *Vickers hardness tester*

The hardness test results are shown in Fig. 14. Four distinguishable zones from left to right can be read from Fig. 14: Fusion zone, CGHAZ, FGHAZ, tempering zone and base metal. Since the same welding electrode was used in the welding program, the average hardness in the fusion zones of both materials is almost the same. Away from the fusion zone, after a sudden drop (near distance=0), the hardness rapidly raises to the peak of the HAZ (CGHAZ) and subsequently decreases to a level lower than both the fusion zone and base metal (FGHAZ, or soft zone). Further is the tempering zone, whose hardness is similar to that of the base metal and thus is difficult to define the boundary between this zone and the base metal.

It should be noted that although the hardness variation patterns of RQT-S690 and S385 are similar, the values are significantly different. Even the highest hardness value in the HAZ is lower than that of the RQT-S690 base metal, while the maximum hardness of the TMCP-S385 is 27.6% higher than that of the TMCP-S385 base metal. From Fig. 14, it can also be seen that the total area contributed by the hardness of the CGHAZ is larger than that of the FGHAZ. As a result, the overall hardness of the HAZ of TMCP-S385 turns out to be higher than the base metal, while the hardness of the HAZ of RQT-S690 is much lower than the base metal. This conclusion is in accordance with the strength alteration shown in Figs. 6 and 7, while the ductility decrease is mainly contributed by the brittle CGHAZ.

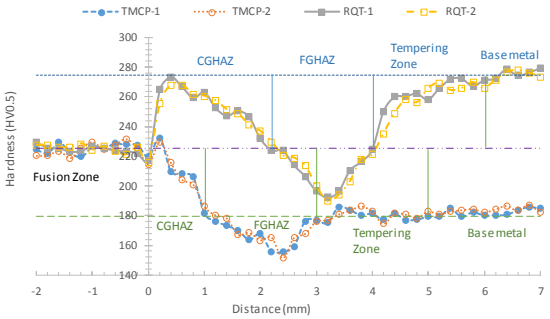

Fig. 14: *Hardness in the HAZ*

3 INFLUENCE OF HAZ ON THE TENSILE PERFORMANCE OF T-STUB JOINTS

3.1 Specimen fabrication

Four T-stub joins were fabricated in this study. Two were made of RQT-S690 16mm plate and the other two were made of TMCP-S385 16mm plate. Each specimen is fabricated by joining two identical steel plates with dimensions of 440×150×16 mm. The joints are designed as *complete penetration butt weld joint* according to the AWS structural steel welding code [23]. Three bolt holes were drilled at each side of the chord plate in order to fix the specimens to the test rig. The distance between two rows of bolt holes (center to center) is 290 mm. The configuration of the joints is shown in Fig. 15. *Flux Core Arc Welding* (FCAW) was employed to finish the welding connection, and the employed electrodes matches the corresponding strengths of each material.

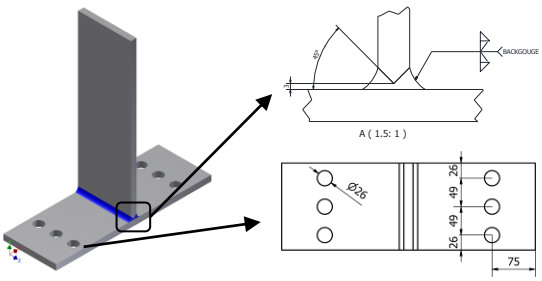

Fig. 15: *Configuration of the T-stub joints*

3.2 Test set-up and testing procedure

Tensile tests for the T-stub joints were carried out in a servo-hydraulic universal test machine that has a maximum loading capacity of 2000kN. To fix the specimen into the test machine, "inverted" support joints made of S355 steel plates with thickness of 50mm were fabricated. The configurations of the support joints are the same as those of the test joints (Fig. 16). The specimens are fixed into the support joints by six M24 high strength hexagon bolts of grade 10.9HR. The full testing set-up is shown in Fig. 16. Since it would be easier to control the testing time, displacement control instead of force control was used during the testing. The loading rate was set as 1mm/min for all time so that quasi-static response could be obtained.

Fig. 16: *The T-stub joint test setup*

3.3 Test results

3.3.1 General behaviour

Fig. 17 presents the test results in terms of the load-displacement curves of the RQT-S690 and TMCP-S385. Despite that the specimens may fail in different modes at different loadings, these curves are of the same pattern. In general, three stages in the load-displacement curves can be distinguished: (1) the elastic stage, (2) plastic hinge stage and (3) the failure stage. In the elastic stage, the stiffness and the elastic modulus govern the behaviours of the joints until yielding takes place. Within this stage, the load increases rapidly with a high load/displacement ratio, which depends on the stiffness of the joint that in turn depends on the material and configuration. When the specimens are further loaded, plastic deformation appears and four obvious plastic hinges could be seen, as shown in Fig. 18. Two of the plastic hinges would appear near the weld toe, and the other two would be near the bolted area. In this stage, the deformation grows more rapidly but the resistance of the joint increases slowly. If the loads are further increased, further hardening will appear due to the large deformation of the joint that change the original configuration of the joint from T to Y shape. Meanwhile, large tensile forces will be induced in the flanges of the T-stub joints and the parallel relationship in the load-displacement curves tends to be disturbed. The final failure usually happened in the forms of either weld toe through thickness fracture or bolt hole necking failure (net section failure under tension).

3.3.2 Design plastic resistance

For design purpose, the behaviour of the joints under the elastic stage and the first yield resistance is of the most importance. To quantitatively evaluate the effects of these two parameters, the elastic stage and plastic hinge stage of the curves are taken out and simplified into a straight line model (Fig. 19). The intersection of the two straight lines or the turning point of the model is defined as the first yield resistance, which is widely accepted as the design plastic resistance of the joint before large deformation appears [24, 25].

In EC3, to estimate the design resistance of T-stub joints, three failure modes, namely (1) complete yielding of the flange, (2) bolt failure with yielding of the flange and (3) bolt failure [25] are identified. In this study, all the specimens were failed by complete yielding of flange. To predict the design resistance of a T-stub joint when it is failed in complete yielding of the flange, two methods based on the yield line analysis are adopted, as specified by EC3 [25].

Method 1: $$F = \frac{4M_{pl,1,Rd}}{m} \quad (1)$$

Method 2: $$F = \frac{(8n-2e_w)M_{pl,1,Rd}}{2mn-e_w(m+n)} \quad (2)$$

In Eqns. 1 and 2, $M_{pl,1,Rd} = l_{eff}(\frac{t}{2})^2 f_y$ is the design moment resistance of the section. l_{eff} is the effective width of the T-stub flange of the joint (Fig. 6.2 of [12], 150mm in this study), m, n are geometrical parameters of the T-stub joints (Fig.20). e_w is either equal to 1/4 of the washer diameter or the width across points of the bolt head of nut, as relevant [12]. Note that in Method 2, instead of concentrated at the center line of the bolt, it is assumed that the force applied to the T-stub flange by a bolt is distributed uniformly under the washer (or the bolt head/nut). Since the distance between the center lines of the weld toe plastic hinge and the bolt area plastic hinge is smaller than m (especially at the beginning of the plastic hinge development stage as shown in Fig. 18), this assumption leads to higher but more realistic resistance.

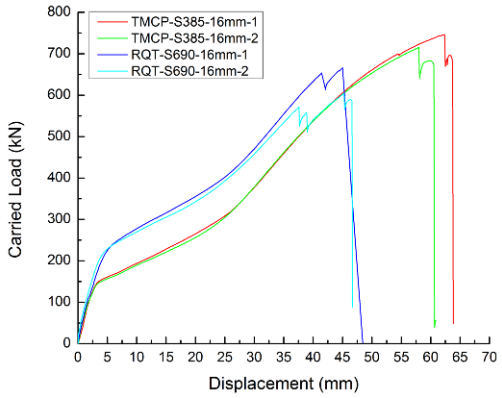

Fig. 17: *Load-displacement curves of the T-Stub joints*

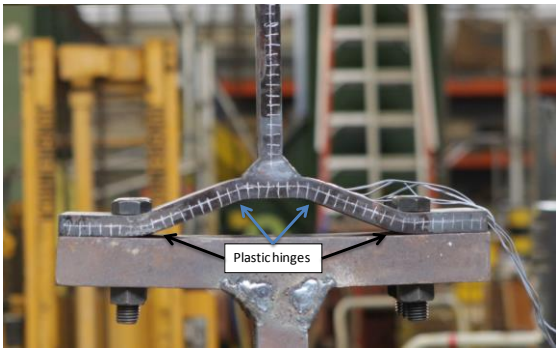

Fig. 18: *Plastic hinges formation*

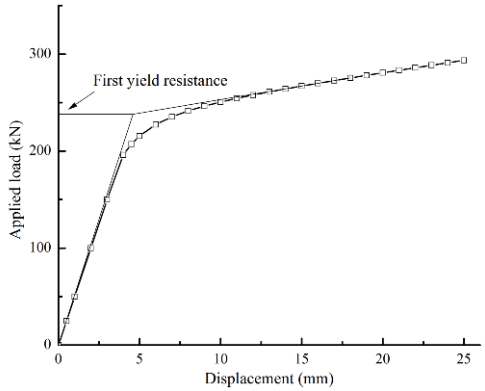

Fig. 19: *Simplified elastic-plastic load-displacement curve*

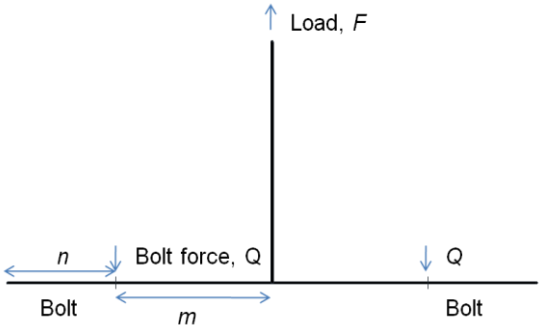

Fig. 20: *Force diagram for T-stub joints*

The design resistance of the studied T-stub joints obtained by Eqns. 1 and 2 and the actual resistance obtained from tests are shown in Table 3. Table 3 shows that the design resistances of the RQT specimens are superior when compared with the TMCP specimens. The average design resistance of 16mm RQT-S690 specimens is about 91.3% more than that of 16mm TMCP-S385 specimens.

Compared with the EC3 equation predictions, the test results of the TMCP specimens are approximately 23% and 14.6% higher than Eqns. 1 and 2, respectively. However, the test results of the RQT-S690 specimens are generally lower than anticipation. The RQT-S690 specimens are only slightly higher than Eqn. 1 and surprisingly lower than Eqn. 2. Based on these test results, it appears that the EC3 equations are conservative when predicting the design resistance for the TMCP-S385 joints but not for the RQT-S690 joints. In fact, these results are in accordance with the welding affected tensile test (Figs. 6 and 7) and Vickers hardness test results (Fig. 14) as well. Therefore, it can be concluded that the influence of HAZ on the strength of TMCP-S385 is negligible or even slightly helpful, but welding reduces the strength of RQT-S690 seriously in the HAZ and eventually shows an impact on the global performance of welded joints.

Table 3: *Design plastic resistance of the tested T-stub joints*

	Test Results (kN)			EC3 Eqns. (k N)		Diff 1(%)	Diff 2 (%)
	Test1	Test2	Ave.	Eqn. 1	Eqn. 2		
RQT-S690	217.8	219.5	218.7	210.3	225.6	4.0	-3.1
TMCP-S385	146.5	142.0	144.3	117.3	125.9	23.0	14.6

For Eqns. 3 and 4, the nominal yield strengths are used. That is, f_y=690 and 385 MPa for RQT-S690 and TMCP-S385, respectively.
Diff 1 = ((Average-Eqn. 3)/Eqn. 3)×100%
Diff 2 = ((Average - Eqn. 4)/Eqn. 4)×100%

4 Conclusions

The influence of welding on the strength of the reheated, quenched and tempered (RQT) high strength steel in grade S690 and the thermo-mechanically controlled processed (TMCP) normal strength steel in grade S385 are investigated in two phases experimental study.

Phase I examined the stress-strain behaviour of the welding heat affected coupons and microstructure and hardness of the heat affected zone (HAZ). It is found that welding may cause serious deterioration in both strength and ductility of RQT-S690, while the strength of TMCP-S385 increases slightly at the expense of ductility. From the fusion zone to the base metal, three sub-HAZs can be distinguished. The coarse grained HAZ shows relatively high hardness; the fine grained HAZ shows relatively low hardness; and the tempering zone has comparable hardness to the base metal. It should be

noted that the average hardness of the HAZ of RQT-S690 is much lower than the base metal, while that of the TMCP-S385 is comparable to the base metal.

Phase II investigated the tensile performance of welded T-stub joints that made of those two materials. The first yield resistances from the test results and the design plastic resistances obtained by using prediction equations provided by EC3 are compared. It is shown that the load carrying capacities of RQT-S690 are below the upper bound of EC3, while test results of the TMCP specimens are much higher than EC3. Further discussion deducts that the problem comes from the compromised properties of the plastic hinges at the weld toe, which is seriously affected by welding heat input.

ACKNOWLEDGEMENT

This research is supported by the Singapore Ministry of National Development (MND) Research Fund on Sustainable Urban Living (Grant No. SUL2013-4). Any opinions, findings and conclusions expressed in this paper are those of the writers and do not necessarily reflect the view of MND, Singapore.

REFERENCES

[1] R. Bjorhovde, "Development and use of high performance steel," *Journal of Constructional Steel Research*, vol. 60, pp. 393-400, 2004.

[2] W. Yu, Y.-j. Qian, H.-b. Wu, and Y.-h. Yang, "Effect of Heat Treatment Process on Properties of 1000 MPa Ultra-High Strength Steel," *Journal of Iron and Steel Research, International*, vol. 18, pp. 64-69, 2011.

[3] *Welding handbnook, volume 1: welding technology*, Eighth Edition ed. Miami: American Welding Society, 1991.

[4] d. M. B., "The weldability of modern structural TMCP steels," *ISIJ International*, vol. 37, pp. 537-551, 1997.

[5] F. Hochhauser, W. Ernst, R. Rauch, R. Vallant, and N. Enzinger, "Influence of the soft zone on the strength of welded modern HSLA steels," *WELDING IN THE WORLD*, vol. 56, pp. 77-85, 2012.

[6] J. D. Verhoeven, *Steel metallurgy for the non-metallurgist*. Ohio, USA: ASM International, 2007.

[7] H. K. D. H. Bhadeshia and R. W. K. Honeycombe, *Steels: microstructure and properties*, 3th ed. Oxford, United Kingdom: Elsevier Science & Technology, 2006.

[8] A. V. Sverdlin and A. R. Ness, Eds., *Chapter 3: fundamental concepts in steel heat treatment* (steel heat treatment handbook: metallurgy and technology. Taylor & Francis Group, 2007, p.^pp. Pages.

[9] J. Outinen, "Mechanical properties of structural steel at elevated temperatures and after cooling down," in *10th International Conference on Fire and Materials 2007, January 29, 2007 - January 31, 2007*, San Francisco, CA, United states, 2007, pp. FM Global; Fire Testing Technology (FTT); SwRI - Dep. Fire Technol., Chem. Chem. Eng. Div.

[10] X. Qiang, F. S. K. Bijlaard, and H. Kolstein, "Post-fire mechanical properties of high strength stuctural steels S460 and S690," *Engineering Stuctures*, vol. 35, pp. 1-10, 2012.

[11] J. C. Golondrino, G. A. MacRae, A. Abu, J. G. Chase, G. W. Rodgers, B. Fu, *et al.*, "Post-fire hysteretic behavior of asymmetrical friction connections," presented at the Proceedings of the 10th pacific structural steel conference, Singapore: Singapore Structural Steel Society and National University of Singapore, 8-11 October 2013.

[12] M. S. Zhao, S. P. Chiew, and C. K. Lee, "Post weld heat treatment for high strength steel welded connections," *Journal of Constructional Steel Research*, vol. 122, pp. 167-177, 2016.

[13] S. Machida, H. Kitada, H. Yajima, and A. Kawamura, "Extensive application of TMCP steel plates to ship hulls: 40 kgf/mm2 class high yield stress steel," *Marine Structures*, vol. 1, pp. 219-243, 1988.

[14] M. Militzer, "1.10 - Thermomechanical Processed Steels," in *Comprehensive Materials Processing*, S. H. F. B. J. V. T. Yilbas, Ed., ed Oxford: Elsevier, 2014, pp. 191-216.

[15] BSI, "hot rolled products of structural steels: part 6 technical delivery conditions for flat products of high yield strength structural steels in the quenched and tempered condition, BS EN 10025-6," ed. London: British Standards Institution, 2004.

[16] D. Kaplan and G. Murry, *Thermal, Metallurgical and Mechanical Phenomena in the Heat Affected Zone*. Kokoken, USA: John Wiley & Sons, 2008.

[17] BSI, "BS EN 10002-1: tensile testing of metallic materials: part1 method of test at ambient temperature," ed. London: British Standards Institution, 2001.

[18] G. E. Linnert, "Welding Metallurgy." vol. Volume 1, Fundamentals, 4th ed Miami, Florida, USA: American Welding Society, 1994.

[19] U. J.S., G. C.M., and G. J.E., "Numerical and experimental analysis of microstructure evolution during arc welding in armor plate steels," *Journal of Materials Processing Technology*, vol. 2009, pp. 1688-1700, 2009.

[20] A.Takahashi and H. Ogawa, "Influence of softened heat affected zone on stress oriented

hydrogen induced cracking of a high strength line pipe steel," *ISIJ International*, vol. 35, 1995.
[21] B. K. Choudhary, J. Christopher, D. P. Rao Palaparti, E. Isaac Samuel, and M. D. Mathew, "Influence of temperature and post weld heat treatment on tensile stress–strain and work hardening behaviour of modified 9Cr–1Mo steel," *Materials & Design*, vol. 52, pp. 58-66, 2013.
[22] BSI, "ISO 6507-1: Metallic materials – Vickers hardness test – Part 1: Test method," ed. London: British Standards Institution, 2005.
[23] AWS, "Structural Welding Code," in *steel*, ed. Miami: American National Standards Institue, 2008.
[24] A. M. Girão Coelho and F. S. K. Bijlaard, "Experimental behaviour of high strength steel end-plate connections," *Journal of Constructional Steel Research*, vol. 63, pp. 1228-1240, 2007.
[25] BSI, "Eurocode 3: design of steel structures: part 1-8 design of joints, BS EN 1993-1-8," ed. London: British Standard Institution, 2005.